Domain Wall Collision-Induced Spin Waves

Tristan Delaney

Massachusetts Institute of Technology, Department of Materials Science and Engineering, 77 Massachusetts Ave, Cambridge, MA 02139

Abstract

A series of micromagnetic simulations are conducted whereby two transverse domain walls are injected into a straight magnetic nanowire under an applied field. It is found that, based on the relative orientation of the domain walls, the two may annihilate, resulting in the generation of an intense spin-wave burst. Since the applied magnetic fields for these simulations are smaller than the Walker breakdown field, these results present an extremely low-energy means of generating and controlling spin waves for engineering applications.

Keywords: spin waves, Landau-Lifschitz-Glibert Equation, magnetic domain walls, magnonics

1. Introduction

1.1 Spin Wave Fundamentals

The temporal evolution of the magnetization vector M(r) in a material is given by the Landau-Lifschitz-Gilbert (LLG) Equation,

$$\frac{d\hat{m}}{dt} = -\gamma\left(\hat{m}\times\vec{H}\right)+\alpha\left(\hat{m}\times\frac{d\hat{m}}{dt}\right) \quad (1)$$

where α is the phenomenological damping constant, γ is the gyromagnetic ratio, $\boldsymbol{m}$ is the unit magnetization vector, and $\boldsymbol{H}$ is the effective field comprised of the exchange, dipolar, anisotropic, and external applied fields acting upon M. In this paper, only the exchange, dipolar, and external fields and their associated energies are taken into account to accurately model permalloy, a soft magnetic material. The exchange field arises from nonzero gradients in the magnetic configuration of lattice moments in the crystal structure of a magnetic material. The dipolar field, also known as the demagnetizing field, arises when "free poles" – magnetic moments which orient themselves orthogonal to a surface – emit stray fields outside of the material itself; the dipolar field usually forces magnetic moments in magnetic media to orient themselves such that stray fields are kept inside the media itself, often at the expense of exchange or anisotropic energies. The experimental value of α is usually measured to be of order 0.01 for soft magnetic materials. The LLG Equation describes the nature of the precession of each lattice moment as it aligns with the sum of all effective magnetic fields presently acting on them. Spin waves (SWs) are collective excitations of these lattice moments that propagate through a magnetic medium, leading to the redistribution of energy introduced into a ferromagnetic system due to external excitation (e.g. an external Oersted field) or internal changes of the topological spin texture within a ferromagnetic structure. SWs were first observed as resonant microwave modes of the magnetization in ferrite samples[1] The nature of these modes was later derived analytically by Walker[2] for spheroids and Damon and Eschbach[3] for ferromagnetic slabs, in the long-wavelength limit of strictly dipolar modes by simultaneously solving Equation 1 together with Maxwell's Equations. In both works, only dipole-dipole interactions are taken into account as this allows one to analytically derive the nature of the resonant modes; thus the modes have a long-wavelength, low frequency character which makes them only applicable on the scale of several millimeters. Thus, many of the applications for these resonant modes in ferrite have been in the areas of measurement and material characterization,[11] antennae,[12] and other applications where a characteristic length of more than a few micrometers is desired.

Recently, interest in spin waves has shifted to higher frequency, shorter wavelength modes that are on the scale of several nanometers. These SWs arise from exchange-dipole and purely exchange modes in high-moment metallic ferromagnets with frequencies of tens to hundreds of GHz depending on the geometry and material parameters of the medium through which they propagate. The short wavelengths of exchange and dipole-exchange SWs make it necessary to take into consideration the effects of all possible fields acting upon the magnetic moments in a nanostructure, making an analytic result of the general dispersion relation unfeasible without the help of numerical simulations.[6] Due to their large group velocities, these SW modes have potential applications in ultra low power information processing and logic devices[4] based on nanoscale geometrical structures such as nanowire conduits, in which the spin wave modes and propagation characteristics can be precisely engineered. The emerging subfield of "magnonics"[23] seeks to understand and control SW excitations in nanoscale magnetic devices, and is focused on such issues as SW band structure and band-gap engineering,[5,13] predictably and controllably generating SW excitations,[13] and understanding the effects of phase shift of SWs as they propagate through domain walls and other nonuniform magnetic textures.[4,15,16]

A challenge for future applications of high frequency SWs in magnonic devices is overcoming the relatively short attenuation length due to the exponential decay in the amplitude of the SWs as they propagate, imposed by the damping term in Eq. 1. Two general approaches have been proposed to compensate for the effect of attenuation: first, to lower the effective damping through materials engineering or using other interactions such as spin-transfer torques induced by spin-polarized current; or, second, to enhance the efficiency of generating large-amplitude SW excitations such that they can be detected at long distances even with the effects of attenuation. The former is quite difficult to accomplish experimentally due to the intrinsic nature of damping and our rather poor microscopic understanding of the phenomenological damping and term, and the effects of spin-transfer in real materials.[16] The latter approach is experimentally fairly simple in principle, but difficult in practice. The conventional means of high-power excitation of SWs is through the application of a large external Oersted field. This in turn requires a large current to generate the required field, which can be very power demanding and often inefficient. This paper explores the possibility of releasing the energy stored in magnetic domain walls through controlled DW collision and annihilation as a means of generating large amplitude SWs on demand using very low power consumption.

1.2 Domain Wall Structure and Topology

Magnetic domain walls (DWs) are local regions where the magnetization undergoes an abrupt change in direction.[17] In order to understand the mechanisms of DW interactions and annihilation, a thorough analysis of the physical structure and topological properties of DWs must be presented. In macroscopic magnetic materials, DWs serve to lower the magnetic energy of the sample as a whole by minimizing stray fields due to free poles at the surface, which require a large amount of energy to maintain. However, DWs themselves cost energy (due to the exchange interaction that prefers uniformly-oriented magnetization). In smaller structures, especially for structures whose dimensions are less than one micron, DWs become energetically unfavorable and serve only as a transition area between two or more domains of differing magnetization. The internal structure of a DW is highly dependent upon the parameters of the material present and upon the size of the sample. This paper is concerned with quasi-one-dimensional magnetic nanowires of rectangular cross-section: high aspect ratio nanostripes of width w, thickness t, and length L, with L>>w>>t. In such structures, the simplest 180^o DW in a rectangular nanowire typically comes in two variations: a transverse wall (TW), where the internal magnetization of the wall is orthogonal to the magnetization on either side and directed along the width of the nanowire (assuming that the width is considerably larger than the thickness); and a vortex wall (VW), where the internal magnetization of the wall rotates around a single moment known as the vortex core (which is directed orthogonal to the plane of rotation).

The topological properties of these two types are quite different. As much of the internal magnetization of a TW is directed to a hard-axis imposed by the narrow width of the wire, the internal energy due to the demagnetizing field is large compared to that of a VW. On the other hand, the rotation of the internal magnetization of a VW greatly increases its internal exchange energy when compared to that of a TW. These differences in internal energy also affect the dynamics of each wall, which have been studied for quite some time. Especially peculiar is the effect of applied field magnitude on TW motion as small fields (often below 15-25 Oe, depending on the dimensions of the wire) will quickly drive a TW into motion up to the critical Walker breakdown field after which the TW undergoes a slower oscillatory motion, mediated by the periodic nucleation and motion of a vortex core across the domain wall.[18,19]

More important for the purposes of this paper is the presence of a topological "charge" within the DWs, which determines several characteristics including DW pinning, injection, and packing.[8,10,20] Figure 1 details the magnetic configurations of these topological defects along with their winding numbers associated with each defect and the position of each defect for both a transverse and vortex DW. For DWs, the winding numbers of all defects contained within the wall sum to zero; this indicates that each wall is a stable structure, but that energy is stored primarily in each defect which makes up the wall. Like protons and electrons, the interaction between two topological defects is determined by their winding numbers – that is, defects of opposite sign annihilate one another while those of the same sign will preserve their overall structure.[8]

2. Procedure

The simulations are run using the Object-Oriented Micromagnetics Framework (OOMMF), a finite differences micromagnetics package developed at NIST. The overall geometry of the structure is of a 1000x40x10 nm^3 nanowire, initially magnetized in the +x-direction, placed between two 200x200x10 nm^3 nucleation pads each with a vortex core. A cell size of 2.5x2.5x10 nm^3 was used in the simulations with the material parameters resembling those of permalloy (M_s = 8.0x10^5 A/m, A = 1.3x10^{-11} J/m^3). The TWs were

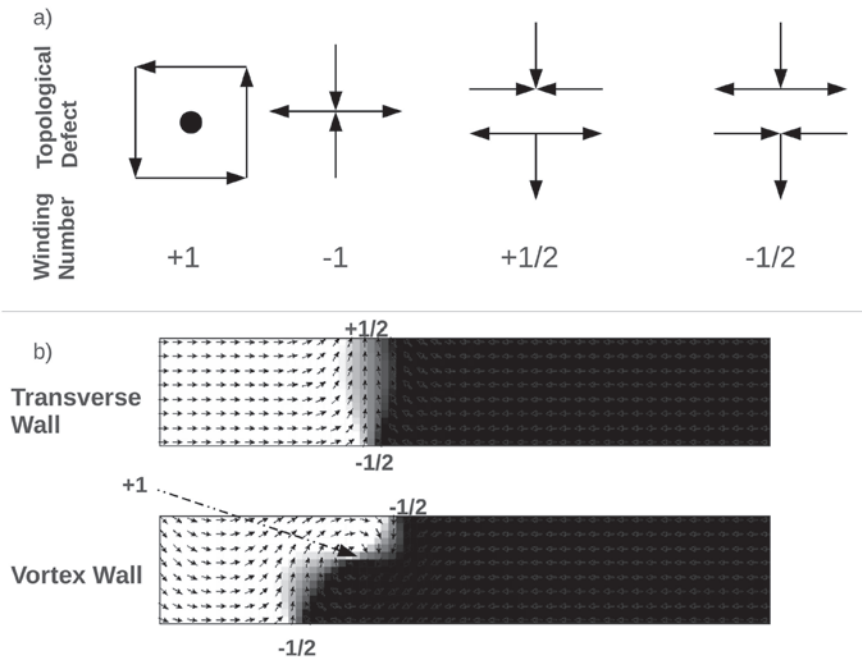

Figure 1: a) Internal and edge defects with associated integer and half-integer winding number b) An example of a transverse wall and a vortex wall. In both cases, the net winding number of the wall is n = 0.

nucleated by applying a 200 Oe field in the –x-direction for approximately 1 nanosecond, after which the applied field was dropped values ranging between 1 and 25 Oe and applied to the system for another 4 nanoseconds. The vorticity of each nucleation pad determines the direction of the internal magnetizations of the injected TWs, and initial configurations of both similar and opposite vorticity are used.

3. Results & Discussion

Controlling the internal magnetization of a TW is found to be very simple as the internal magnetization is determined by the magnetization of the part of the vortex adjacent to the beginning of the nanowire. Thus, nucleation pads of the same vorticity nucleate TWs of opposite internal magnetization while pads of opposite vorticity nucleate TWs of the same internal magnetization. Thus, SWs can only be generated if the nucleation pads are of opposite vorticity (Figure 2).

Another set of simulations was run to compare the amplitude of SWs generated using a powerful Oersted field. Using the same geometry and material parameters, but not nucleating any DWs into the nanowire beforehand, an Oersted field was applied to a row of cells in the center of the wire in the z axis in the form of a sine cardinal function,

$$H_Z = H_{MAX} \frac{\sin(2\pi\nu t)}{2\pi\nu t} \quad (2)$$

where ν = 100 GHz and H_{MAX} ranged between 100 Oe and 10 kOe. The sine cardinal function serves to equally excite all modes of SWs up to 100 GHz and its dispersion relation gives all possible modes allowed in the geometry. The dispersion relations were determined by calculating the Discrete Fourier Transform of the z-component (out of plane) magnetization for a 400 nm line of cells within the middle of the nanowire for 2 nanoseconds after the external Oersted field was applied, and are plotted on a logarithmic scale since the Fast Fourier Transform (FFT) power of all possible modes scales several orders of magnitude. The parabolic relation between frequency (*f*) and wave vector (*k*) is characteristic of the generally dispersive nature of SWs; thus SWs of higher frequency propagate at higher velocities than those of lower frequency. The dispersion relations for H_{MAX} = 100 Oe and H_{MAX} = 10 kOe, shown in Fig 3(a-b), show that all of the modes up to 50 GHz are equally excited, and that the FFT power of these modes rises in proportion to the value of H_{MAX}.

In contrast with those generated by the external Oersted Field, the SWs generated via TW annihilation using a 1 Oe and 25 Oe field, Fig 3(c-d), show very little differences in the FFT powers of the SW modes generated. The data show that the TW annihilation scheme produces SWs ranging between 12 and 50 GHz in a nearly uniform population of allowed modes, all of extremely large amplitude. The uniformity of the SWs generated, regardless of the magnitude of the driving field, shows that these modes generated are directly related to the energy stored in the magnetic configurations of the TWs themselves. This result has great implications on the efficiency of TW annihilation as a means of generating SWs, compared to the conventional externally applied field

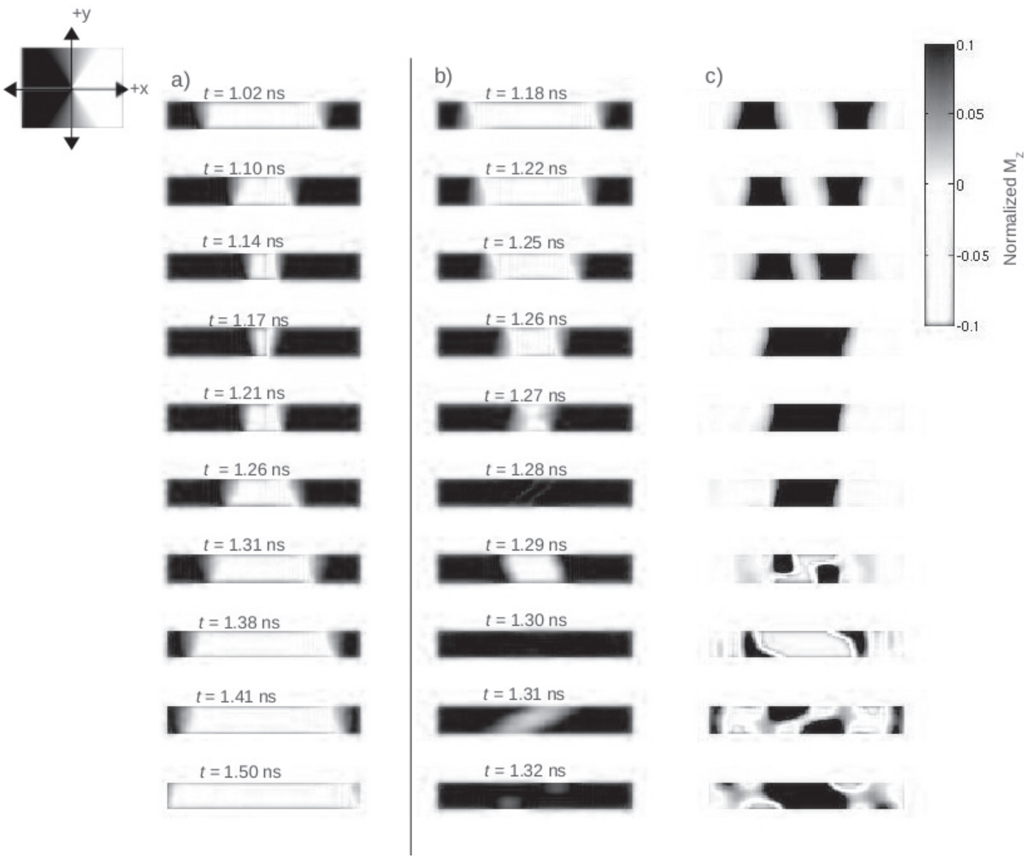

Figure 2: Side by side comparison of the collision between TWs of various internal magnetizations: a) opposite (-y/+y) and b) similar (+y/+y). c) When two walls are of the same internal magnetization, their topological defects of opposite winding number annihilate generating large amplitude SWs.

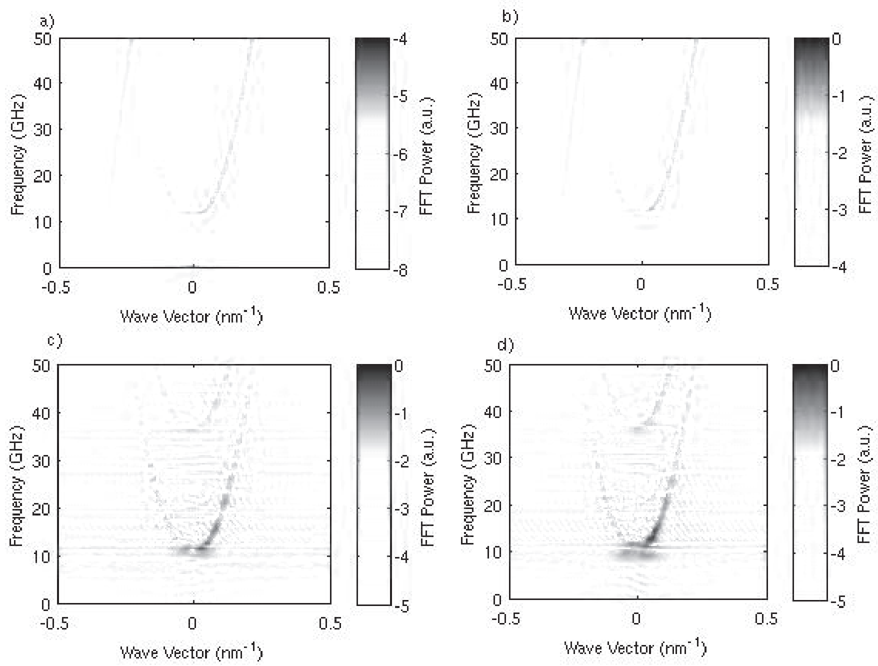

Figure 3: Dispersion relations for sine cardinal Oersted fields with H_{MAX} = 100 Oe (a) and H_{MAX} = 10 kOe (b) as well as TW collision induced SWs at driving fields of H_d = 1 Oe (c) and H_d = 25 Oe (d).

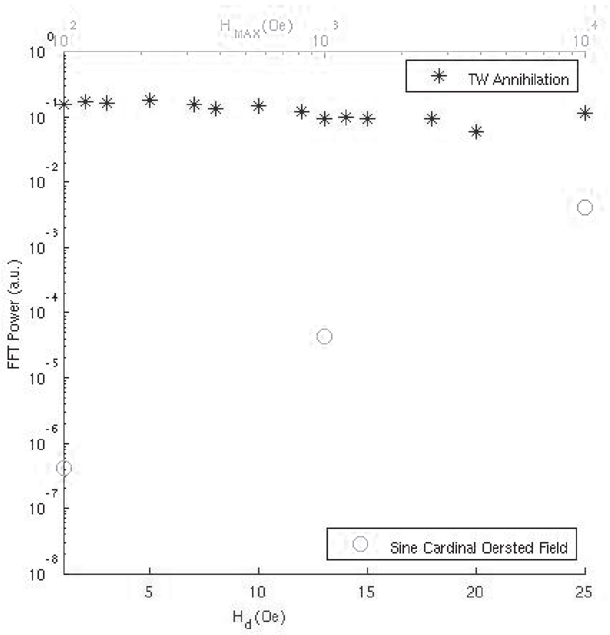

Figure 4: Comparison of FFT Power of the two methods.

as most TWs only require minimal field to actually drive their motion.

The extreme advantage of this method, however, lies in the amplitude of the SWs generated for extremely low power input. Figure 4 compares the FFT power of the SW packet with k = 0.1133 nm^{-1} and f = 21 GHz for both TW annihilation-induced SWs and the Oersted fields. As was stated before, SWs generated via TW annihilation are largely the same in amplitude regardless of the strength of the applied field; however, this is not true for the Oersted fields which require an extremely large applied field in order to excite large amplitude SWs. Yet even with the large field, the SWs generated by the Oersted fields pale in comparison to the ones generated by the annihilation of the TWs (Figure 4).

The key to generating large amplitude, high frequency SW pulse lies in the efficiency with which energy can be stored within the magnetic moments and transmitted through SWs. For the method proposed in this paper, the energy in the system is stored in the exchange and dipolar energy in a nucleated TW. These energy components are released upon annihilation at the collision site of the two TWs, which serves as a high energy oscillatory region which continuously generates SWs until it has relaxed to an equilibrium state. However, for the applied Oersted field, energy is introduced into the system solely through the Zeeman interaction of the applied field with the moments subjected to the field. The maximum Oerstead field that could be experimentally generated is of order 10 kOe using a microelectromagnet, and only hundreds of Oe using the fringing fields from current-carrying excitation wires. By contrast, the effective exchange fields within a DW are of order 10^3-10^4 kOe, and is independent of the driving field that propels the domain walls together. This effect is also supported by the SWs generated by TW annihilation whose overall nature is not affected by the magnitude of the driving field.

The means of inserting energy into the system for both methods contrast heavily in terms of efficiency. The applied Oersted field requires an extremely large amount of power to simply generate a magnetic field large enough to generate SWs, but in the experimental setting, this would require large amounts of current to generate this field only to produce extremely small SWs. However, for the nucleation of two TWs, the field required can be lowered to as low as 20 Oe, based on changes to geometry of the nanostructure into which the walls are injected. After the TW is generated, the only external field necessary is one strong enough to drive a TW across a wire, which requires a field of less than 1 Oe for soft magnetic materials such as permalloy. The results show that higher fields only serve to minimize the time of TW annihilation so long as the field is below the Walker breakdown field of the wire.

4. Conclusion

This paper presents an efficient and generally simple means of generating SWs by controlling the orientation of two TWs so that they will annihilate upon contact. Using the large densities of exchange and dipolar energies stored in the wall, the method proposed generates large amplitude SWs which remain of reasonable size even in the presence of attenuation over large distances. Due to the fact that the SWs generated are characteristic of the internal energy structure of a TW, their amplitude and dispersion relation are uniform regardless of the external field applied – thus a small field-driven collision generates the same SWs as does a field near the Walker breakdown threshold of the TW. Once again, the size of the external field necessary to generate SWs using TW annihilation makes this method much more power efficient than the conventional means of generating SWs in the lab, which requires a large Oersted field which, in turn, requires a large current. The amplitude of the SWs generated via TW annihilation is also much larger than those generated by an external field, and this could allow for the easier study of nonlinear behavior of SWs which cannot normally be done without extremely high applied fields. The crucial element of this method lies in the control of the orientation of the TW, as only TWs of the same internal magnetization will actually annihilate and create SWs, but several means of controlling TW orientation have been suggested and confirmed by simulation. Overall, this method provides a promising solution which takes advantage of the selective nature of TW topology and uses this energetically unfavorable structure as a means of reliably generating large amplitude SWs which can then be used for study or application.

Acknowledgements

Funding support through the MIT Undergraduate Research Opportunities Program (UROP) is gratefully acknowledged. The author would like to thank Professor Geoffrey Beach for his support and contributions to this paper.

References

1. White, L.R.; Solt, I.H. Physical Review Letters **1956**, 104, 56-62.

2. Walker, L. R. Physical Review Letters **1957**, 105, 390-399.

3. Damon, R. W.; Eshbach, J. R. Journal of Physics and Chemistry of Solids **1961**, 19, 308-320.

4. Hertel, Ricardo; Wulfhekel, Wulf; Kirschner, Jürgen. Physical Review Letters **2004**, 93, 257202

5. Lee, K.; Han, D.; Kim, S. Physical Review Letters **2009**, 102, 127202.

6. Soohoo, R.F. Physical Review Letters **1960**, 120, 1978-1982

7. Atkinson, D.; Eastwood, D.S.; Bogart, L. K. Applied Physics Letters **2008**, 92, 022510

8. Kunz, A. Applied Physics Letters **2009**, 94, 13502

9. Lee J.; Lee, K; Choi, S.; Guslienko, K.; Kim, S. Physical Review B **2007**, 76, 184408.

10. Kunz, A.; Reiff, S. Applied Physics Letters **2009**, 94, 192504.

11. Chen, L.; Ong, C.K.; Neo, C.P.; Varadan, V.V; Varadan, V.K. Microwave electronics: measurement and materials characterization; John Wiley & Sons: West Sussex, 2000.

12. Lee, S.; Kim, Y.; Lee, J.; Kim, S.; Krylov, S. K. Samsung Electronics Co., Ltd. Active Magnetic Antenna with Ferrite Core. U.S. Patent 20090289860, November 26, 2009.

13. Barman, A. Journal of Applied Physics D: Applied. Phyics **2010**, 43, 195002.

14. Choi, S.; Lee, K.; Yu, K.; Guslienko; Kim, S. Physical Review Letters **2007**, 98, 087205.

15. Choi, S.; Lee, K.; Kim, S. Applied Physics Letters **2006**, 89, 062501.

16. Seo, S.; Lee, K.; Yang, H.; Ono, T. Physical Review Letters **2009**, 102, 147202.

17. Zhang, S.; Li, Z. Physical Review Letters **2004**, 93, 127204.

18. O'Handley, R. Modern Magnetic Materials; John Wiley & Sons: New York, 2000.

19. Beach, G.; Nistor, C.; Knutson, C.; Tsoi, M.; Erskine, L. Nature Materials. **2005**, 4, 741-744.

20. Porter, D.; Donahue, M. Journal of Applied Phyics **2004**, 95, 6729-6731.

21. Atkinson, D.; Eastwood, D.; Bogart, L. Applied Physics Letters **2008**, 92, 022510.

22. Tretiakov, O.; Tchernyschyov, O. Physical Review B **2007**, 75, 012408.

23. Kruglyak, V. V.; Demokritov, S. O.; Grundler, D. Magnonics. Journal of Applied Physics D: Applied. Phyics **2010**, 43, 264001.

About the Author

Tristan Delaney graduated with a Sc. B. in Mathematics from MIT in 2011 and continued onto a PhD in Computational Applied Mathematics at Stony Brook University in New York. His research focus is on mesh generation, computational geometry and finite element analysis. Contact at: tdelaney@ams.stonybrooke.edu.